



Identification of rainy periods from ground based microwave radiometry

Ada Vittoria Bosisio, Ermanno Fionda, Patrizia Basili, Giovanni Carlesimo & Antonio Martellucci

To cite this article: Ada Vittoria Bosisio, Ermanno Fionda, Patrizia Basili, Giovanni Carlesimo & Antonio Martellucci (2012) Identification of rainy periods from ground based microwave radiometry, European Journal of Remote Sensing, 45:1, 41-50, DOI: [10.5721/EuJRS20124505](https://doi.org/10.5721/EuJRS20124505)

To link to this article: <http://dx.doi.org/10.5721/EuJRS20124505>



© 2012 The Author(s). Published by Taylor & Francis.



Published online: 17 Feb 2017.



Submit your article to this journal [↗](#)



Article views: 19



View related articles [↗](#)



Citing articles: 1 View citing articles [↗](#)

Identification of rainy periods from ground based microwave radiometry

Ada Vittoria Bosisio^{1*}, Ermanno Fionda², Patrizia Basili³, Giovanni Carlesimo⁴
and Antonio Martellucci⁵

¹CNR/IEIT c/o DEI -Politecnico di Milano, Milano (Italy)

²Fondazione Ugo Bordoni, Roma (Italy)

³University of L'Aquila, Dept of Electrical and Information Engineering, L'Aquila (Italy)

⁴University of Perugia, Dept. of Electronics and Information Engineering, Perugia (Italy)

⁵European Space Agency, ESTEC, TEC-EEP, Noordwijk (Netherlands)

*Corresponding author, e-mail address: bosisio@elet.polimi.it

Abstract

In this paper the authors present the results of a study aiming at detecting rainy data in measurements collected by a dual band ground-based radiometer.

The proposed criterion is based on the ratio of the brightness temperatures observed in the 20-30 GHz band without need of any ancillary information. A major result obtained from the probability density of the ratio computed over one month of data is the identification of threshold values between clear sky, cloudy sky and rainy sky, respectively. A linear fit performed by using radiometric data and concurrent rain gauge measurements shows a correlation coefficient equal to 0.56 between the temperature ratio and the observed precipitation.

Keywords: Microwave radiometry, rain monitoring, tropospheric propagation.

Introduction

Ground-based radiometers are used to investigate the sky thermal emissions in order to retrieve geophysical observables such as the total amount of water vapor (PWV), the non-precipitating cloud liquid content (LWC) and the zenith wet delay (ZWD). These atmospheric parameters are very useful in several fields such as global and climate change, radio astronomy study, space geodesy and Earth-space telecommunication projects [Turner et al., 2007]. Besides, the radiometric data all weather availability and their acquisition rate (up to 1 Hz) make it possible to perform a high-time resolution analysis almost continuously.

Long-term analysis of sky thermal emissions (T_b 's), from single ground-based microwave radiometers during massive measurement campaign or from radiometric-networks, could benefit from some analytic criterion to detect data affected by rain events. As well known, brightness temperatures (T_b 's) measured, at the ground, at 20-30 GHz under rainy conditions are not appropriate to retrieve the above-mentioned quantities [Ware et al., 2004].

The identification of rainy period is of importance also for the telecommunication systems operating at Ka and Q/V bands, where a major impairment derives from the effect of the lowest layers of the atmosphere on radio-wave propagation.

The knowledge of the atmospheric condition along the propagation path could avoid the

implementation of high fixed power margin and favour the adoption of adaptive fade mitigation technique [COST255, 2002; de Monteiro et al., 2010].

Hence, the aim of this work is to identify a criterion for data quality control, a flag to be used in real-time or quasi real-time. Specifically, the final goal is to detect whether measurements are taken under scattering phenomenon (rain) or non scattering phenomenon. As well known, brightness temperatures given by ground-based radiometers are derived through the radiative transfer equation under the scatter-free assumption [Ulaby et al., 1981].

For ground-based radiometry, in the absence of an efficient and reliable automatic tool to remove data affected by rainy events, a strong help comes from concurrent data observed by co-located rain gauge.

Due to the response of microwave radiometric channels (at 20-30 GHz), which have a different sensitivity to the atmospheric constituents, a possible way to detect rainy radiometric data could be based on the ratios between pairs of T_b 's.

The ratio between T_b 's appears more suitable as an indicator than the single channel brightness temperature itself to discriminate sky conditions. In fact, a linear relationship between T_b 's jointly measured around 20 and 30 GHz exists under clear sky condition, while it becomes strongly non linear in the presence of heavy clouds or rain events [Mallet and Lavergnat, 1992]. Also, it is observed that specific temperature ratio values can be related to different atmospheric scenarios, ranging from clear to rainy sky [Bosisio and Capsoni, 1995].

In this paper the authors present the preliminary tests of the criterion performance. The analysis is referred to the experimental radiometric and rain gauge data collected during April 2008 in Cabauw (NL), in the framework of the Dutch CESAR Project. In Cabauw are long operating a large set of remote sensing instruments such as 3-channel ground-based microwave radiometer (with channels at 21.3, 23.8 and 31.65 GHz), rain gauges, ceilometer, GPS, radiosounds and meteo-radar [Fionda et al., 2008].

Modelling Background

The authors briefly recall the relationship between brightness temperature values (T_b in K) and PWV, denoted by V [mm], while the reader is referred to [Bosisio and Capsoni, 1995] for further details. Under clear sky, the brightness temperature could be expressed as:

$$T_b(f_i) = a_i V + b_i \quad [1]$$

where a_i [K mm⁻¹] and b_i [K] are frequency- and elevation angle-dependent coefficients and f_i is the radiometric frequency [GHz]. The coefficient values are the result of a linear fitting based on a large radio sounding database and concurrent radiative transfer forward modelling [Bosisio and Mallet, 1994]. It follows that the relationship between the two T_b observed at the two operative radiometric channels, namely 23.8 and 31.65 GHz (in the following referred to as T_{b23} and T_{b31}), becomes:

$$T_{b31} = c_0 \cdot T_{b23} + c_1 \quad [2]$$

with $c_0 = a_{31}/a_{23}$ and $c_1 = b_{31} - b_{23} \cdot (a_{31}/a_{23})$.

The ratio T_{b31}/T_{b23} depends on the state of the atmosphere, but the same ratio value needs a proper modification to be related to the path condition effectively. As a matter of fact, eq. [1] strictly holds in clear sky. The presence of liquid along the propagation path affects the brightness temperature values of an amount that depends on the frequency. Under cloudy or rainy sky this leads to an ambiguity hidden in eq. [2] and related to the quantity V of water in vapour phase. As a countermeasure against this possible effect, one could refer to the *unbiased* brightness temperature T'_{b31} :

$$T'_{b31} = T_{b31} - c_1 \quad [3]$$

which is not affected by the contribution of the water vapour plateau. The two temperature values T_{b31} and T_{b23} are related by a direct proportionality law. The criterion to detect rainy measurements is based on the values of the ratio indicator R :

$$R = T'_{b31}/T_{b23} \quad [4]$$

that is the constant of proportionality. It helps us to describe the sky condition along the path without additional tools.

The discrimination capability of the ratio R was also tested by other experimenters [Luini et al., 2007] without further inspection. Here, the authors aim at assessing on a statistical basis the relationship between R and the values of the rain content [mm].

Experimental data

The results presented in this paper refer to a dataset of one month of radiometric and rain gauge data collected during April 2008 in Cabauw (NL), in the framework of the Dutch CESAR Project.

Specifically, measurements are collected by a 3-channel ground-based microwave radiometer developed by RESCOM (Aalborg, DK) and designed for automatic unattended operation. The sampling rate is 0.25 Hz and the path elevation angle is 60°. Rain intensities are collected every hour in 4 locations surrounding the station.

The time series of the brightness temperature values are shown in Figure 1 together with the concurrent rain gauge measurements. NI240, NI260, NI344 and NI350 are the acronyms for the 4 rain gauges.

As it appears, the chosen dataset is probably not the most favourable for rain monitoring, as the rainy events are few in number and weak in intensity. Nevertheless, it was chosen for the validation in this preliminary phase as this dataset quality was fully tested in previous experiments [Fionda et al., 2008].

Preliminary data analysis

The relationship between the temperature values T_{b31} and T_{b23} is shown by the scatter diagram in Figure 2, where the grey dots highlight data with concurrent rain gauges measurements. The solid black line depicts the linear relationship between the two temperature values - see [1] and [2] -, where the coefficients $c_0 = 0.35$ (dimensionless) and $c_1 = 7.8$ [K] are obtained from data.

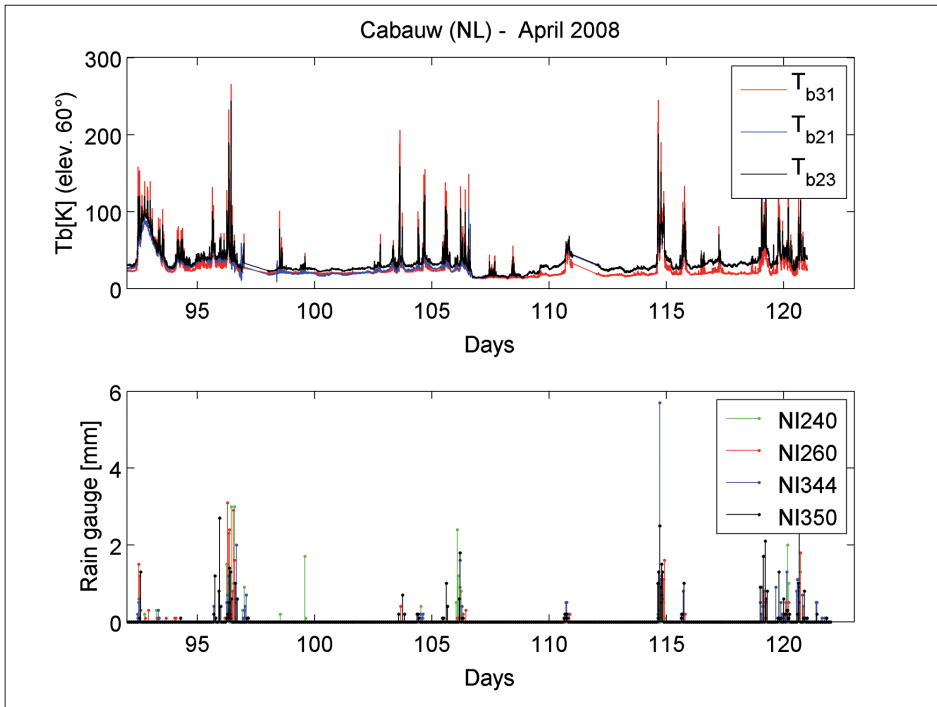


Figure 1 - The data set under test: measured brightness temperatures at 21.3, 23.8 and 31.65 GHz (a) and rain gauge data (b). NI240, NI260, NI344 and NI350 are the acronyms for the 4 rain gauges.

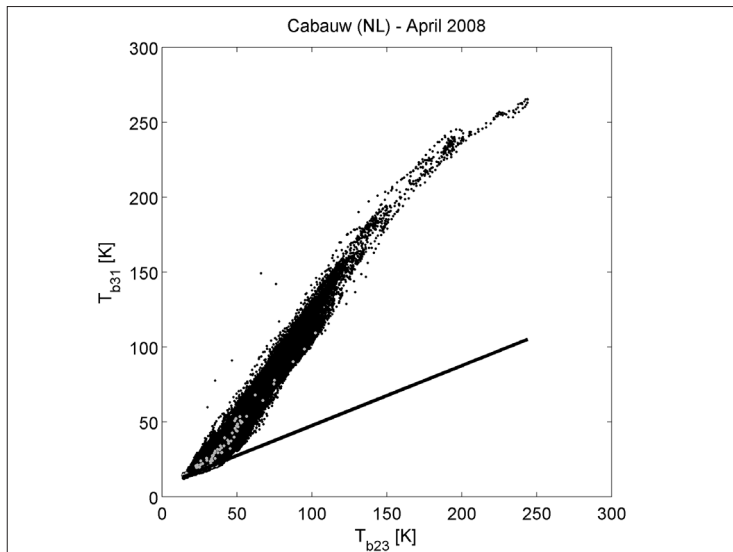


Figure 2 - Scatterplot between measured T_{b31} and T_{b23} . The whole dataset is shown in black, while measurements at the time instants of concurrent rain gauges data are shown in grey.

The scatter plot shows that rain measurements taken every 1 hour are not useful to infer about the presence, the actual intensity and duration of the rain event along the propagation path. Besides the different sampling rate, this point is related to the proper functioning of the two instruments: the radiometer collects an integral value that depends - among other parameters - on the atmospheric conditions along the whole propagation path, while the rain gauge - due to the space-time structure of the precipitation field - collects values along a sampling path that is distributed according to the fall trajectory of the rain. For the same amount of precipitation, an intense shower results in brightness temperatures higher than those of an event with lower intensity but longer duration.

A criterion based on the time instant values of the temperature could encompass this intrinsic weakness.

The ratio R , as defined in [4], is shown together with its time derivative, after proper low-pass filtering and decimation (1 sample every 30 minutes), in Figure 3. It can be noticed that R is sensitive to the brightness temperature raise due to the presence of rain or liquid along the path, while it is almost constant under clear sky.

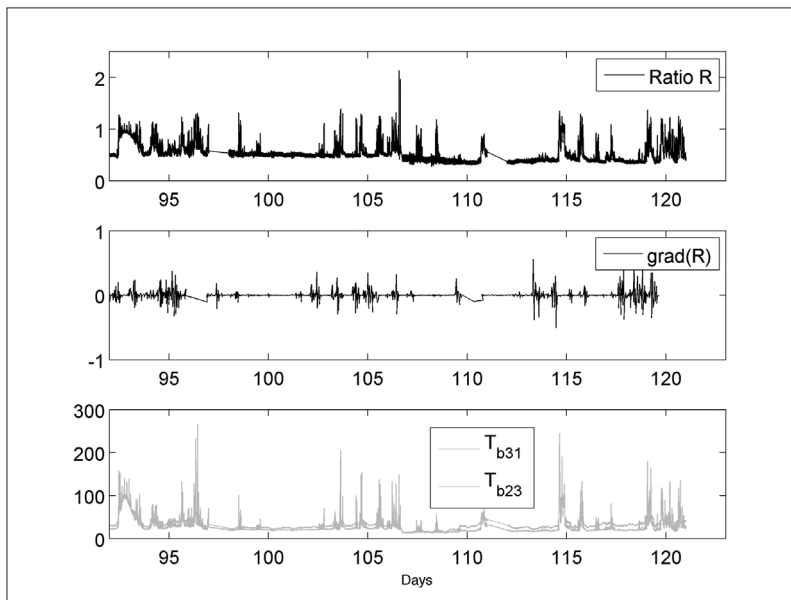


Figure 3 - Discrimination capabilities of R : from top to bottom R time series, R time derivative, T_{b23} and T_{b31} time series.

Twelve rainy events were detected from concurrent but not co-located rain gauges measurements and from visual inspection of the temperature time series. In Figure 4 the rainy-events are depicted in grey.

An event-based analysis reveals that the relationship between R and T_{b31} changes according to the amount of liquid content or rain along the path. Figure 5 illustrates in the leftmost panels two subsets from the 12 selected events chosen as representative of possible rainy conditions along the propagation path, while the rightmost panel shows the scatter plot of

all 12 rainy periods. It is to underline that since the location of the rain gauges is not precisely known (a) and that the rain intensity values are collected every 1 hour (b), the identification of possible rain events is not that precise. Nevertheless, the ratio R seems to have two different trends, one referred to *light-medium rain* (white line) condition and a second one referred to rainy condition (grey curve) as shown in the rightmost panel of Figure 5.

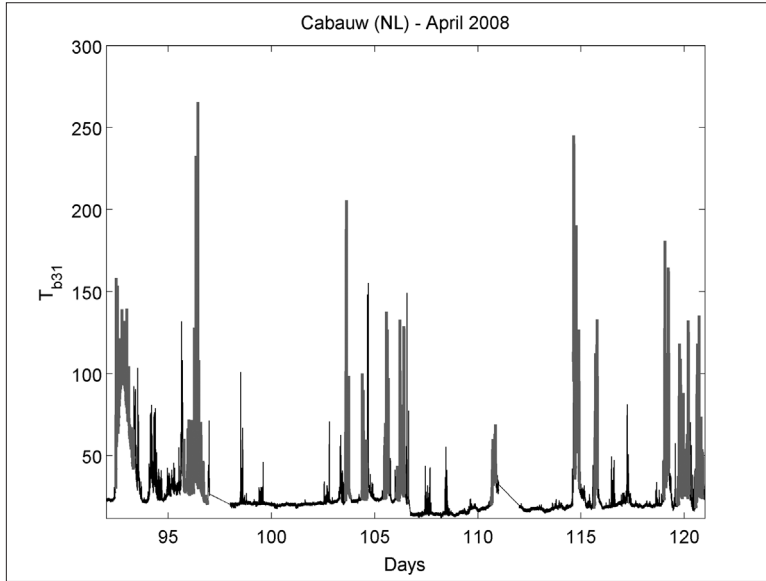


Figure 4 - Time series of measured T_{b31} (black line). The rainy events are shown in grey.

A regression analysis was performed over the dataset by means of a linear fit on the dataset characterized by T_{b31} values < 60 K and of a second-order polynomial fit on the remaining data. The linear regression applied to the cloudy sky ($T_{b31} < 60$ K) has the following expression:

$$R = 0.0112 \cdot T_{b31} + 0.2260 \quad [5]$$

with correlation coefficient $\rho = 0.84$ and $RMSE = 0.061$. The polynomial regression of 2nd order valid for rainy data ($T_{b31} > 60$ K) is:

$$R = -2.5 \cdot 10^{-5} \cdot T_{b31}^2 + 9 \cdot 10^{-3} T_{b31} + 0.41 \quad [6]$$

with correlation coefficient $\rho = 0.79$ and $RMSE = 0.043$.

Numerical Results

Besides a behavioral analysis of the ratio indicator, the key interest is the relationship between the ratio and the precipitation as a criterion to exclude rainy data for atmospheric retrieval or, conversely, to detect them for the adoption of dynamic fade mitigation techniques (FMT).

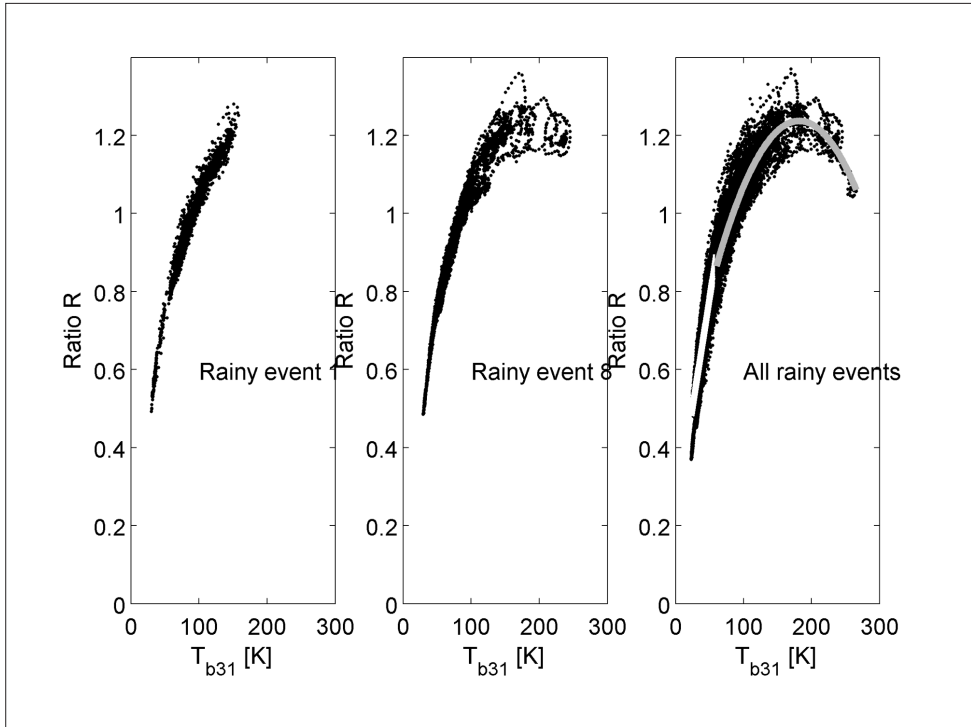


Figure 5 - Scatter plots between R and T_{b31} during *rainy* events: (from left to right) light rain event; medium/heavy rain event; all rainy events. The white line and the gray curve are representative of the two type of precipitation intensity.

The plot of the probability density of R in Figure 6a shows 3 peak values that could be interpreted as thresholds between clear sky, cloudy sky and rainy sky, respectively (see Tab.1). These three different regions/behaviours are barely visible in the probability density curve of T_{b31} value (Fig. 6b). The CDF plots reveal these thresholds in term of different slope regions (Figs 6c and 6d).

Table 1 - Sky conditions: R and T_{b31} threshold values.

	R	T_{b31} [K]
Clear sky	0.3 ÷ 0.5	11 ÷ 25
Cloudy sky	0.5 ÷ 0.8	25 ÷ 60
Rainy sky	>0.8	>60

The ratio R seems to be a good indicator of the atmospheric condition along the observation path. The strong correlation value between R and T_{b31} is not surprising as, by definition through eq. [4], the two quantities are not independent. The use of the ratio R , instead of the single temperature T_{b31} emphasizes the effect of the three different path conditions on the instrument response (see Figs. 6a and 6b). Nevertheless, the discrimination capability of R has to be proved against completely independent measurements such as brightness

temperatures collected at a frequency sensitive to the rain (in the Ku band) or rain precipitation data. Because of the lack of a line between 13 and 15 GHz, the validation was performed through a linear fit between the rain gauge data and the 1 hour average R values. The regression analysis was performed by choosing as independent quantity in one case the mean values of the precipitation and in a second case the maximum one. The motivation of this choice is twofold: firstly, the location of the four rain gauges is not exactly known with respect to the radiometer one; secondly, the wind direction is not known. This implies that the direction of the incoming rain event is not known.

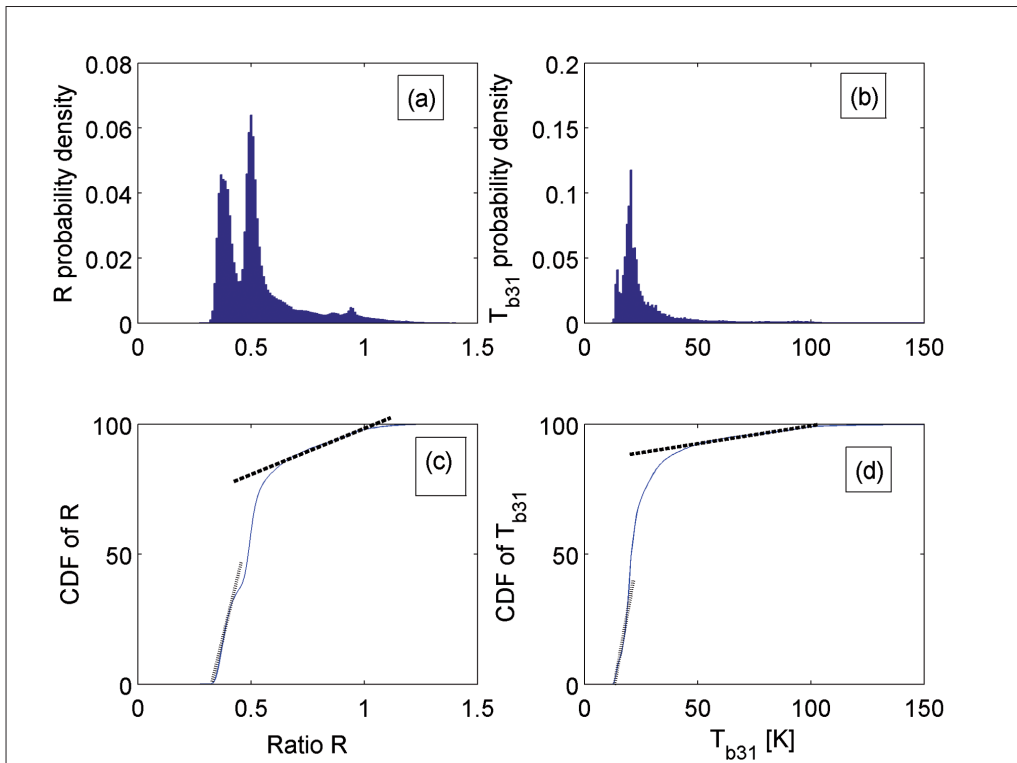


Figure 6 - Statistical characteristics: probability density of R (a) and T_{b31} (b); cumulative distribution of R (c) and T_{b31} (d).

As there is no reason to assess a main role to one of the four rain gauges, we considered either the average measured values or the maximum one. It is to remind that the radiometer is sensitive to the atmospheric condition all along the observation path, while the rain gauge measurement is a punctual one. Notwithstanding this intrinsic difference between the measured quantities, the results of the linear fit are promising. The regression lines are shown in Figure 7. According to the correlation coefficient value the best fit is between the ratio R and the mean rain gauge measurement ($\rho = 0.56$ instead of $\rho = 0.533$ when considering the maximum value), while the RMSE values are almost the same (0.1327 in the first case instead of 0.1323 in the second one).

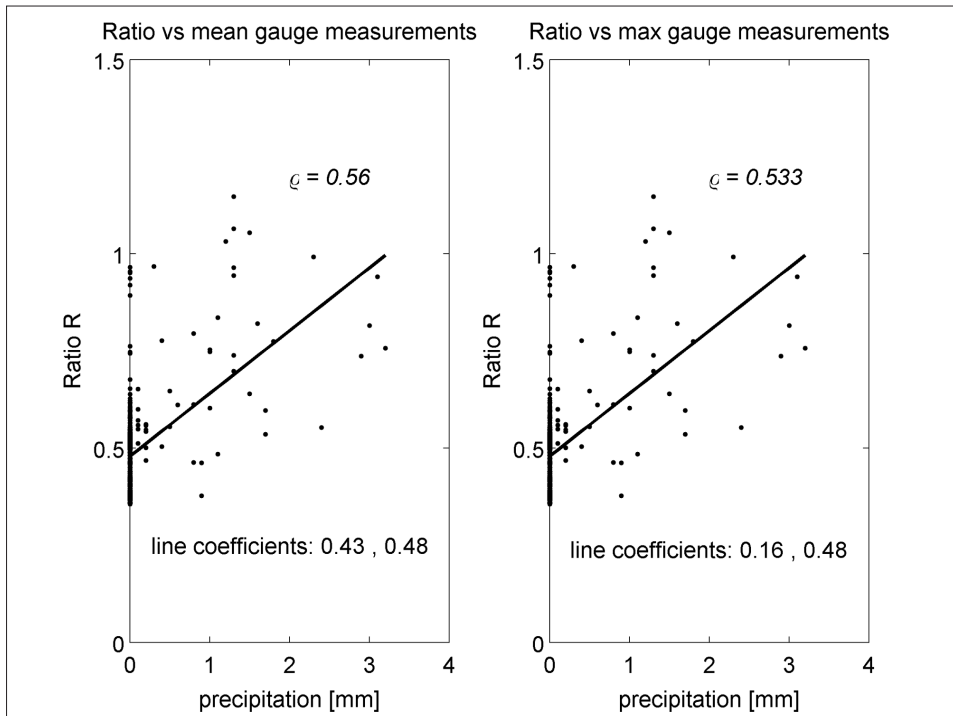


Figure 7 - Regression analysis over the ratio R and the measured rain precipitation by considering the mean value (left) and the maximum one (right).

Conclusions

The detection of rainy-sky radiometric data is of importance for both remote sensing applications and telecommunication needs. In the former case it avoids misleading retrieval of water vapour or liquid content along the observation path, while in the latter it could support the adoption of adaptive fade mitigation techniques.

The proposed criterion based on an unbiased ratio between brightness temperatures measured at 23.8 and 31.65 GHz proved to be a useful tool towards this goal.

The ratio R seems to be a good indicator of the atmospheric condition along the observation path. The promising results of this preliminary analysis need to be confirmed against a larger dataset. Besides, the knowledge of both the rain gauges exact location and the azimuth angle of the radiometer observation path will contribute to the refinement of the analysis.

The encouraging performances of the ratio indicator R need to be confirmed on both a longer temporal basis and different sites to single out a season- or location-dependent behavior, if any.

Acknowledgements

The authors would like to thank Prof. Piero Ciotti (Dept. of Electrical and Information Engineering, University of L'Aquila,) and Dr. Stefania Bonafoni (Dept. of Electronics and Information Engineering, University of Perugia) for their useful suggestions. Also, the authors are grateful to the referee for its helpful comments.

References

- Bosisio A.V., Mallet C. (1994) - *A three frequency non linear algorithm for water vapor and liquid water content retrieval*, PIERS 94, Progress in Electromagnetics Research Symposium-ESTEC Centre, Noordwijk (NL), 11-15 July.
- Bosisio A.V, Capsoni C. (1995) - *Effectiveness of brightness temperature ratios as indicators of atmospheric path conditions*, Microwave Radiometry and Remote Sensing of Environment. (Editor: D. Solimini), VSP, Utrecht (NL), pp. 129-138, ISBN 90-6764-189-8.
- COST 255 (2002) - *Radiowave propagation modelling for new satcom services at Ku-band and above*, COST 255 Final Report, Chapter 5.3, ESA Publications Division, SP-1252.
- Fionda E., Basili P., Bonafoni S., Mattioli V., Ciotti P., Martellucci A. (2008) - *Retrieval algorithms of atmospheric parameters using thermal emission observed by surface-based microwave radiometer operated in Cabauw*, ESA Workshop on Radiowave Propagation 2008, Noordwijk (NL), December 3-5.
- Luini L., Riva C., Capsoni C., Martellucci A. (2007) - *Attenuation in non rainy conditions at millimeter wavelengths: assessment of a procedure*, IEEE Transactions on Geoscience and Remote Sensing, 45 (7): 2150-2157. doi: <http://dx.doi.org/10.1109/TGRS.2007.895336>.
- Mallet, C., J. Lavergnat (1992) - *Beacon calibration with a multifrequency radiometer*, Radio Science, 27 (5): 661-680. doi: <http://dx.doi.org/10.1029/92RS00817>.
- de Montera L., Barthès L., Mallet C., Golé P., Marsault T. (2010) - *Assessment of rain fade mitigation techniques in the EHF band on a Syracuse 3 20/44-GHz low elevation link*, Comptes Rendus Physique, 11 (1): 18-29. doi: <http://dx.doi.org/10.1016/j.crhy.2009.12.002>.
- Turner D.D., Clough S.A., Liljegren J.C., Clothiaux E.E., Cady-Pereira K.E., Gaustad K.L. (2007) - *Retrieving liquid water path and precipitable water vapor from the Atmospheric Radiation Measurement (ARM) Microwave Radiometers*, IEEE Transactions on Geoscience and Remote Sensing, 45 (11): 3680-3690. doi: <http://dx.doi.org/10.1109/TGRS.2007.903703>.
- Ulaby F.T., Moore R.K., Fung A.K. (1981) - *Microwave Remote Sensing Active and Passive, Vol. 1: Microwave Remote Sensing Fundamentals and Radiometry*, Addison-Wesley.
- Ware R., Cimini D., Herzegh P., Marzano F., Vivekanandan J., Westwater E. (2004) - *Ground-based microwave radiometer measurements during precipitation*, Proc. 8th Specialist Meeting on Microwave Radiometry, 24-27 Feb, Rome, Italy.

Received 17/02/2011, accepted 19/10/2011

© 2012 by the authors; licensee Italian Society of Remote Sensing (AIT). This article is an open access article distributed under the terms and conditions of the Creative Commons Attribution license (<http://creativecommons.org/licenses/by/4.0/>).